VOL. 13, NO. 14, JULY 2018 ISSN 1819-6608
ARPN Journal of Engineering and Applied Sciences

www.arpnjournals.com

THE ADRC LINEAR POWER CONTROL APPLIED TO THE WIND TURBINE SYSTEM BASED ON DFIG

Issam Minka[1], Ahmed Essadki[1] and Tamou Nasser[2]
[1]Higher Normal School of Technical Education, Mohammed V University, Rabat, Morocco
[2]Higher National School of Computer Science and Systems Analysis, Mohammed V University, BP, Rabat, Morocco
E-Mail: issamminka@gmail.com

ABSTRACT

This paper present the model and test of the robustness of the linear Active Disturbance Rejection Control (ADRC) applied to the Doubly Fed Induction Generator (DFIG) inserted in Wind Energy Conversion System (WECS). The objective is to show the tracking of the references and to prove the robustness of this control against internal parameters variations of the DFIG, in order to show their performances. Firstly we start by modeling the components of the Aeolian conversion chain (wind turbine, MPPT strategy, DFIG and the power converters). Thereafter, we study in detail the principle and performance of the ADRC technique used in the control of Rotor Side Converter (RSC) and Grid Side Converter (GSC). Using the Matlab/Simulink environment we present the simulation results of this control and their interpretations.

Keywords: DFIG, ADRC, MPPT, wind turbine.

1. INTRODUCTION

The wind system has become one of the most widely used sources of renewable energy for electric production. This allows researchers to intervene in this field and to innovate several solutions that develop the wind system, the realization of robust and efficient controls applied to the wind-energy conversion chain based on the double-feed induction generator DFIG is one of the solutions that allows the stabilization of the system against variations of the internal parameters of the machine because of the instability of the temperatures which affects the performances of the system, among the methods used the ADRC is one of the robust controls, which can estimate in real time any unexpected disturbance of the controlled system due to its Extended State Observer (ESO) [1, 2], so all disturbances are estimated and rejected in real time.

The wind chain conversion is structured as follow:

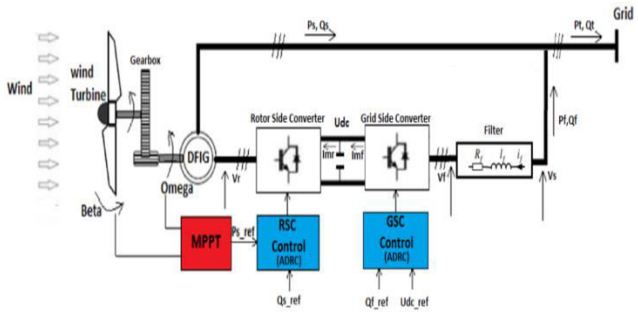

Figure-1. Structure of the WECS.

In this paper, we present the model of the WECS components which are presented in the "Figure-1" (Wind turbine, DFIG, the power converters "RSC and GSC"). After that, we study in detail the controls applied to this chain conversion which are: MPPT, the ADRC control which is applied to the rotoric currents of RSC, the DC link voltage and to the filter currents of GSC.We conclude by presenting the simulation results of these controls and their interpretations.

2. MATHEMATICAL MODEL OF THE AEOLIAN CONVERSION CHAIN

2.1 Wind turbine

The turbine transforms the captured kinetic energy into a torque that rotates the rotor shaft; this phenomenon is expressed by the aerodynamic power P_{aer} and the turbine torque T_t according to the characteristic of the turbine given by the Betz law [3]:

$$P_{aer} = \frac{1}{2} C_p(\lambda, \beta).S.\rho.V^3 \quad (1)$$

$$T_t = \frac{P_{aer}}{\Omega_t} = \frac{1}{2} C_p(\lambda, \beta).S.\rho \frac{V^3}{\Omega_t} \quad (2)$$

With S is a circular surface swept by the turbine, ρair density, V represent the wind speed and $C_p(\lambda, \beta)$ is the power coefficient that represents the characteristic of the turbine:

$$C_p(\lambda, \beta) = 0.5176\left(\frac{116}{\lambda'} - 0.4\beta - 5\right)\exp\left(\frac{-21}{\lambda'}\right) + 0.0068\,\lambda \quad (3)$$

$$\text{With:} \quad \frac{1}{\lambda'} = \frac{1}{\lambda + 0.08\beta} + \frac{0.035}{\beta^3 + 1} \quad (4)$$

Or β is the pitch angle, λ is the ratio of the speed is given by:

$$\lambda = \frac{\Omega_t R}{V} \quad (5)$$

The curves of the power coefficient $C_p$as a function of λ for different values of β are represented in "Figure-2":

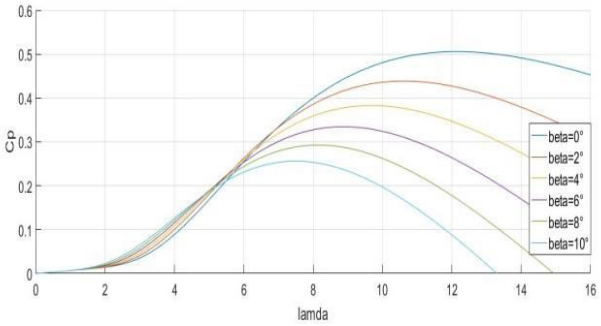

Figure-2. Simulation of the power coefficient$C_p(\lambda,\beta)$.

As the "Figure-3" shows the shaft of the turbine connected to the DFIG via a multiplier with a coefficient G, aims to adapt the turbine speed to that required by the generator. The total inertia Jconsists ofthe turbine inertia J_t andthe generator shaftinertiaJ_g. In order to establish the progress ofthe mechanical speedΩ_{mec}, we apply the fundamental equation of the dynamics from the total torque applied to the rotor we find [6]:

$$\Omega_{mec} = \frac{1}{f+Jd/dt}(T_g - T_{em}) \quad (6)$$

With: $J = J_g + J_t.G^2$ (7)

$$T_g = T_m + T_{em} + f.\Omega_{mec} \quad (8)$$

Or f is coefficient of viscous friction,$T_m$and T_{em} are respectively mechanical and electromagnetic torque.

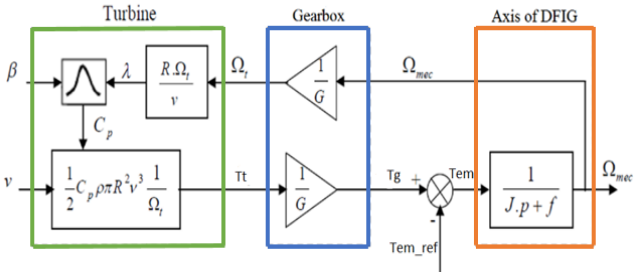

Figure-3. The diagram block of the wind turbine.

2.2 Model of the DFIG

To do a simple model of double fed induction generator, we chose a Park reference linked to the rotating field. The generator power is high, then the stator resistance R*s* is negligible [6, 9]and the stator flux $\emptyset_s$ is oriented along the axis d and is constant in permanent regime:

$$\emptyset_{sd} = \emptyset_s = L_s i_{sd} + M i_{rd} \quad (9)$$

$$\emptyset_{sq} = L_s i_{sq} + M i_{rq} = 0 \quad (10)$$

$$\emptyset_{rd} = \sigma L_r i_{rd} + \frac{M}{L_s}\emptyset_{sd} \quad (11)$$

$$\emptyset_{rq} = \sigma L_r i_{rq} \quad (12)$$

$$V_{sd} = R_s i_{sd} + \frac{d\phi_{sd}}{dt} = 0 \quad (13)$$

$$V_{sq} = R_s i_{sq} + w_s \phi_{sd} = w_s \phi_s = V_s \quad (14)$$

$$V_{rd} = R_r i_{rd} + L_r.\sigma\frac{di_{rd}}{dt} - g w_s \sigma L_r i_{rq} \quad (15)$$

$$V_{rq} = R_r i_{rq} + l_r.\sigma\frac{di_{rq}}{dt} + g w_s L_r \sigma i_{rd} + g w_s \frac{MV_s}{w_s L_s} \quad (16)$$

Where $\sigma = L_r - \frac{M^2}{L_s}$: dispersion coefficient.

The expressions of active and reactive power are given as follows:

$$P_s = -\frac{M}{L_s} i_{rq} V_s \quad (17)$$

$$Q_s = V_s\frac{\emptyset_s}{L_s} - V_s\frac{M}{L_s} i_{rd} \quad (18)$$

The electromagnetic torque of the DFIG is written as follows:

$$T_{em} = p\frac{M}{L_s}\emptyset_{sd} i_{rq} \quad (19)$$

From the established equations, we can find the relations between the generator statoric powers and the voltages applied to the rotor of the machine, which gives the functional diagram of the DFIG presented in The "Figure-4".

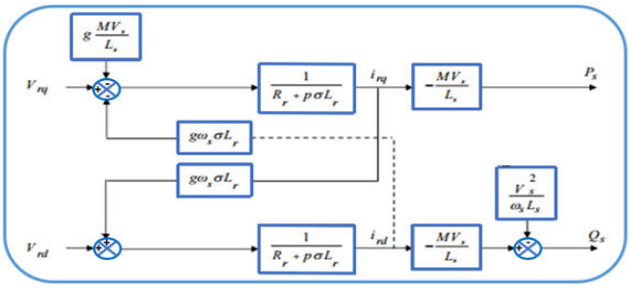

Figure-4. The simplified mathematical model of the DFIG.

2.3 The power converters, the DC link and the RL filter

The "Figure-5" shows the bidirectional power converters (RSC and GSC) connected via the DC bus with capacity C. The goal of the RSC control is to decouple the frequency of the machine from that of the network despite the variations in speed rotation, thereby providing sufficient rotor voltages to provide the necessary torque that is used to vary the mechanical speed of the DFIG to extract the maximum power generated. The GSC connected to the grid by a filter (Rf, Lf), the aim of the control of this converter is to ensure the active power exchange between the rotor and the network, and also to stabilize the DC bus voltage [5].

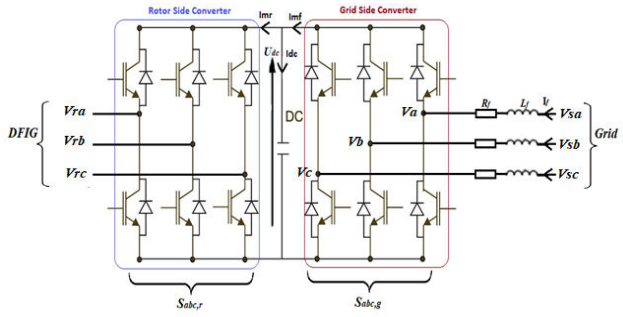

Figure-5. Back to back converter.

$S_{abc,r}$ and $S_{abc,g}$ are switching signals corresponding to the transistors commutators (a, b and c designate the arms and r or g indicate the rotor side or grid side). $I_f$denote the filter current, I_{mf} the current which circulate between the GSC and RSC. $I_{mr}$is a load current of the GSC. The relations between voltage and current are given in d-q axis reference frame as follow [6]:

- **RL filter**

The model of *RL* filter in the three phases is deduced from "Figure-5".

$$\begin{cases} V_a - V_{sa} = (L_f.S + R_f)I_{fa} \\ V_b - V_{sb} = (L_f.S + R_f)I_{fb} \\ V_c - V_{sc} = ((L_f.S + R_f)I_{fc} \end{cases} (20)$$

We apply the park transformation to Equation. (20) we obtain the model d-q of the filter RL:

$$\begin{cases} V_{sd} - V_{fd} = L_f \frac{dI_{fd}}{dt} + R_f I_{fd} + L_f w_s I_{fq} \\ V_{sq} - V_{fq} = L_f \frac{dI_{fq}}{dt} + R_f I_{fq} - L_f w_s I_{fd} \end{cases} \quad (21)$$

With: $\begin{cases} V_{fd} = S_d U_{dc} \\ V_{fq} = S_q U_{dc} \end{cases}$ (22)

Or $S_{d,q}$ indicates switching functions in d-q plan and $U_{dc}$is the DC voltage.

- **The DC bus**

The equations of DC bus are expressed as follows:

$$\frac{dU_{dc}}{dt} = \frac{1}{C}\left(I_{mf} - I_{mr}\right) \quad (23)$$

$$I_{mf} = \frac{3}{2}(I_{fd}S_d + I_{fq}S_q) \quad (24)$$

$$P_f = \frac{3}{2} I_{fq} V_{sq} \quad (25)$$

$$Q_f = \frac{3}{2} I_{fd} V_{sq} \quad (26)$$

With P_f and Q_f are respectively the active and reactive power of grid.We obtain if we neglect losses in power converters:

$$P_f = P_{dc} = U_{dc} I_{mf} \quad (27)$$

We replace the Equation. (25) and Equation. (23) in (27) we find:

$$C U_{dc} \frac{dU_{dc}}{dt} = \frac{3}{2} V_{sq} I_{fq} - U_{dc} I_{mr} \quad (28)$$

3. THE CONTROLS APPLIED TO THE WECS

3.1Maximum power point tracking control MPPT

We make a speed ratioλ to their optimal value $\lambda_{optim}$to adjust the rotational speed of the turbine to capture the maximum of the incident energy at the wind speed [4] [6][7].

The electromagnetic torque reference T_{em_ref} is deduced form an estimate of the wind speed and the mechanical rotation speed [6, 8].

$$P_{aer\_ref} = \frac{1}{2} C_{p\_max}(\lambda, \beta).\pi.R^2.\rho.V^3 \quad (29)$$

$$T_{em\_ref} = \frac{P_{aer\_ref}}{\Omega_t} = \frac{1}{2} C_{p\_max}(\lambda, \beta).\pi.\rho.\frac{R^5.\Omega_t{}^3}{\lambda_{optim}{}^3} \quad (30)$$

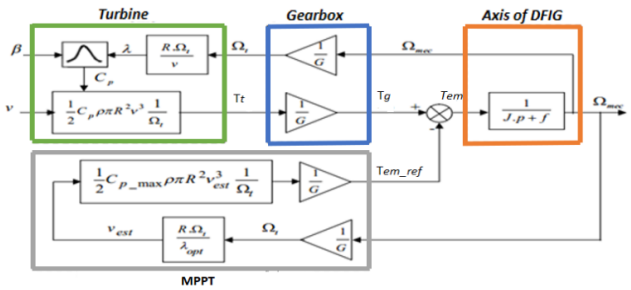

Figure-6. Block diagram of MPPT.

3.2 Active disturbance rejection control

Han found a new robust control in 1995 called Active Disturbance Rejection Control (ADRC); this command is based on proportional corrector and an Extended State Observer ESOthat allows observing any unexpected perturbation of the system controlled and compensate external and internal disturbances of the system in real time [6].

The cost and time deployed by the researchers to establish a detailed model of the physical system in the equation is reduced because of this ESO observer used [10, 13].

To illustrate the Principle of the ADRC we propose the following first-order system:

$$\dot{f} = u(f, n, t) + b_0 x \quad (31)$$

Where *x* and *f* are input and output of system. *n*is the external disturbance, and $u(f, n, t)$the function which

represents the effect of internal dynamics and external disturbance and b_0 is a parameter to estimate.

The mean idea is the approximation and restitution of *u*. So the Equation. (31) can be written in state space form:

$$\begin{cases} \dot{v}_1 = v_2 + b_0 x \\ \dot{v}_2 = u \\ f = v_1 \end{cases} \quad (32)$$

Or in matrix form:

$$\begin{cases} \dot{v} = Ev + b_0 G * x + Nu \\ f = Hv \end{cases} \quad (33)$$

Where: $E = \begin{bmatrix} 0 & 1 \\ 0 & 0 \end{bmatrix}; G = \begin{bmatrix} 1 \\ 0 \end{bmatrix}; H = \begin{bmatrix} 1 \\ 0 \end{bmatrix}; N = \begin{bmatrix} 1 \\ 0 \end{bmatrix}$.

A state observer of Equation. (32) will estimate all the changes of *f* and *u*,this equation becomes a state in the extended state model [6].

Then the linear extended state observer (LESO) will be modeled as follows:

$$\begin{cases} \dot{y} = Ez + b_0 Gu + L(f - \tilde{f}) \\ \tilde{f} = HywhereL = \begin{bmatrix} \beta_1 \\ \beta_2 \end{bmatrix} \end{cases} \quad (34)$$

L is the gain vector of the observer. To simplify the process of regulation, the observed gains are adjusted as follows: [7]:

$$L = \begin{bmatrix} -2\omega_0 \\ \omega_0^2 \end{bmatrix} \quad (35)$$

Where, ω_0 is the bandwidth of the state observer [7]. An Optimal bandwidth adjustment increases the accuracy of the estimation and reduces the sensitivity to noise. Then a correctly designed ESO, y1 and y2 respectively follow *f* and *u*.

The control law is given by:

$$x = \frac{x_0 - y_2}{b_0} \quad (36)$$

The original function in Equation. (31) is decreasing to a unit gain integrator [6].

$$\dot{f} = (u - y_2) + x_0 \approx x_0 \quad (37)$$

A simple proportional controllercan controlled this.

$$x_0 = K_p(e - y_1) \quad (38)$$

Where, *e* is the reference input to follow.

The regulator is chosen as $K_p = \omega_0$, where ω_0 is the desired frequency pulse [12].

The association of linear ESO and PI controller forms the linear ADRC, and we setω_0=3~10ω_c, and consequently, for an efficient result $\omega_c$is the only parameter to choose [6].

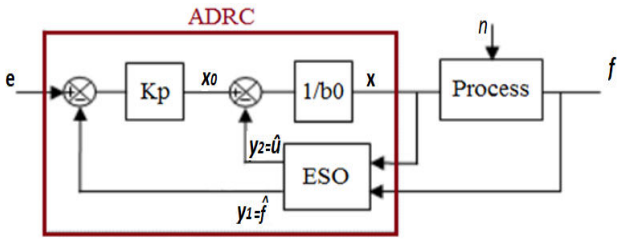

Figure-7. The implementation of the linear ADRC.

4. ADRC APPLIED TO RSC AND GSC

4.1 The ADRC for RSC

From Equation. (15) and Equation. (16), the following expressions of rotor currents are deduced:

$$\frac{di_{rd}}{dt} = -\frac{R_r}{L_r.\sigma} i_{rd} + g w_s i_{rq} + \frac{V_{rd}}{L_r.\sigma} \quad (39)$$

$$\frac{di_{rq}}{dt} = -\frac{R_r}{l_r.\sigma} i_{rq} - g w_s i_{rd} - g\frac{MV_s}{\sigma l_r.L_s} + \frac{V_{rq}}{l_r.\sigma} \quad (40)$$

We put the previous expressions in the form:

$$\frac{di_{rd}}{dt} = u_d(i_{rd}, n, t) + b_0 x \quad (41)$$

$$\begin{cases} u_d = -\frac{R_r}{\sigma L_r} i_{rd} + g\omega_s i_{rq} + (\frac{1}{\sigma L_r} - b_0) V_{rd} \\ x = V_{rd} \ , \ b_0 = \frac{1}{\sigma L_r} \end{cases} \quad (42)$$

$$\frac{di_{rq}}{dt} = u_q(i_{rq}, n, t) + b_0 x \quad (43)$$

$$\begin{cases} u_q = -\frac{R_r}{l_r.\sigma} i_{rq} - g w_s i_{rd} - g\frac{MV_s}{\sigma l_r.L_s} + (\frac{1}{\sigma L_r} - b_0) V_{rq} \\ x = V_{rq} \ , \ b_0 = \frac{1}{\sigma L_r} \end{cases} \quad (44)$$

$u_d$andu_q are the internal and external disturbance affecting respectively the rotor currents $i_{rd}$and i_{rq}. x = $V_{rd}$and$x = V_{rq}$ are the inputs of the currents loops control i_{rd} and i_{rq}. $b_0$is a parameter to define.

We can define the parameters easily K_p , $\beta_1$and $\beta_2$of the ADRC regulators, so the rotor currents track their references $i_{rd_ref}$and i_{rq_ref} which are gives by:

$$i_{rq\_ref} = -\frac{1}{2} C_{p\_max}(\lambda, \beta).\frac{\rho.\pi.L_s.R^5.\Omega_t{}^3}{M.V_s.\lambda_{optim}{}^3} \quad (45)$$

$$i_{rd\_ref} = \frac{\emptyset_s}{M} - \frac{L_s}{M.V_s} Q_{s\_ref} \quad (46)$$

As the "Figure-8" shows the diagram blocks of the ADRC regulators which control the rotor currents, and that prove it is simple to realize.

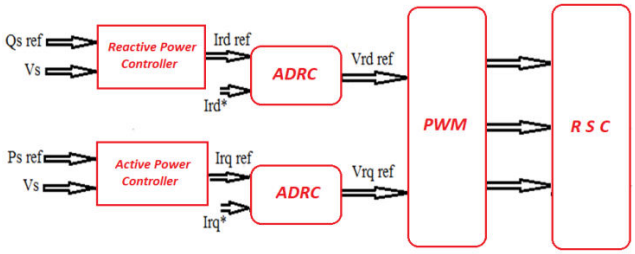

Figure-8. Diagram block for the RSC.

4.2 The ADRC for GSC

- **DC bus control:**

By developing the Equation. (28), we find the following expression of the voltage U_{dc} across capacitor C:

$$\frac{dU_{dc}{}^2}{dt} = \frac{3}{C}V_{sq}I_{fq} - \frac{2}{C}U_{dc}I_{mr} \quad (47)$$

We set $W = U_{dc}{}^2$ the previous equation we find:

$$\frac{dW}{dt} = \frac{3}{C}V_{sq}I_{fq} - \frac{2}{C}\sqrt{W}I_{mr} \quad (48)$$

This equation can also be written as follows:

$$\frac{dW}{dt} = u_W(W,n,t) + b_0 x \quad (49)$$

$$\begin{cases} u_W = -\frac{2}{C}\sqrt{W}I_{mr} + (\frac{3}{C}V_{sq} - b_0)I_{fq} \\ x = I_{fq} \ , \ b_0 = \frac{3}{C}V_{sq} \end{cases} \quad (50)$$

$u_W$presentsthe internal and external disturbance, $W$the input of the DC voltage loops control U_{dc}. $b_0$is a parameter to define.

The values of the parameters of the ADRC regulator K_{pc}, $\beta_{1c}$and β_{2c}, are fixed at precise valuesto maintain the voltage U_{dc} constant.

- **Control of the filter currents:**

From Equation. (21), the following expressions of the filter currents are deduced:

$$\begin{cases} \frac{dI_{fd}}{dt} = \frac{1}{L_f}V_{sd} - \frac{1}{L_f}R_f I_{fd} - w_s I_{fq} - \frac{1}{L_f}V_{fd} \\ \frac{dI_{fq}}{dt} = \frac{1}{L_f}V_{sq} - \frac{1}{L_f}R_f I_{fq} + w_s I_{fd} - \frac{1}{L_f}V_{fq} \end{cases} \quad (51)$$

By putting it in the canonical form of an ADRC regulator, Equation. (51) becomes:

$$\frac{di_{fd}}{dt} = u_{fd}(I_{fd},n,t) + b_0 x \quad (52)$$

$$\begin{cases} u_{fd} = \frac{1}{L_f}V_{sd} - \frac{1}{L_f}R_f I_{fd} - w_s I_{fq} + (\frac{1}{L_f} - b_0)V_{fd} \\ x = V_{fd} \ , \ b_0 = -\frac{1}{L_f} \end{cases} \quad (53)$$

$$\frac{di_{fq}}{dt} = u_{fq}(I_{fq},n,t) + b_0 x \quad (54)$$

$$\begin{cases} u_{fq} = \frac{1}{L_f}V_{sq} - \frac{1}{L_f}R_f I_{fq} + w_s I_{fd} + (\frac{1}{L_f} - b_0)V_{fq} \\ x = V_{fq} \ , \ b_0 = -\frac{1}{L_f} \end{cases} \quad (55)$$

$u_{fd}$and u_{fq} are the internal and external disturbances affecting the rotor currents $I_{fd}$and I_{fq}. $x = V_{fd}$and$x = V_{fq}$ are the inputs of the currents loops control I_{fd} and I_{fq}. $b_0$is a parameter to define.

After having chosen the values of the parameters K_{pf} , $\beta_{1f}$and $\beta_{2f}$of the ADRC controllers, which allows currents of the filter to follow their reference I_{fd_ref} and I_{fq_ref} that can be deduced from Equation. (25), Equation. (26) and Equation. (27):

$$\begin{cases} I_{fd\_ref} = \frac{2}{3V_{sq}}Q_{f\_ref} = 0 \\ I_{fq\_ref} = \frac{2I_{mf}}{3V_{sq}}U_{dc\_ref} \end{cases} \quad (56)$$

The "Figure-9" presents the structure of the ADRC regulators applied to GSC:

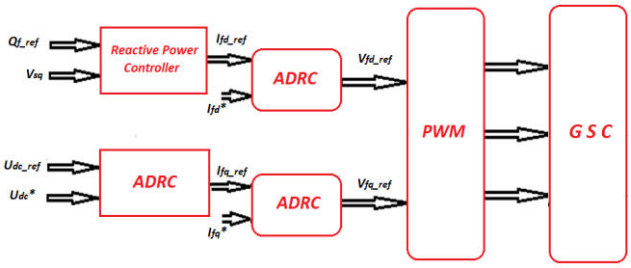

Figure-9. Diagram block for the GSC.

5. SIMULATIONS RESULTS

5.1 Tracking test of the ADRC

In this part, using the ADRC regulator in the transient and permanent regimes, we will test the tracking of the rotor and filter currents as well as the active and reactive powers of their references. The generator operates in hypo-synchronous and hyper-synchronous mode with a mechanical speed of the MADA ranging between 250.4rad/s and 422.7rad/s. The profile of the mechanical speed which follow the profile of wind speed is presented in "Figure-10", which is applied to the blades of the turbine with a pitch angle β=0.

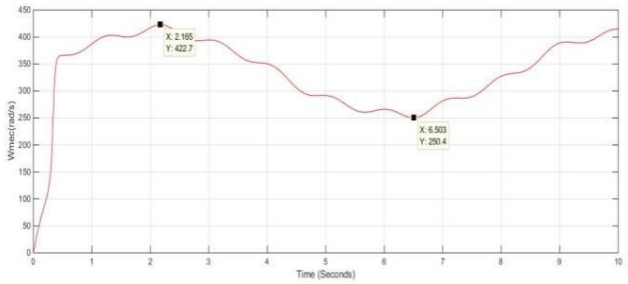

Figure-10. Mechanical speed of the MADA.

From the result obtained on "Figures 11, 12,13 and 14" shows that the tracking of set points is always ensured with using the ADRC control, however the rotor currents as well as for active and reactive powers follow their reference in transit and permanent regime.

According to the results obtained in "Figures 15, 16, and 17", the DC voltage $U_{dc}$and the filter currents follow their references.

We also notice, the coupling between the two direct and quadratic currents has disappeared because of the ADRC.

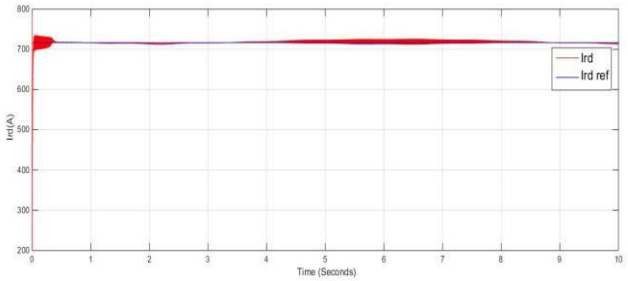

Figure-11. The quadrature rotor currents.

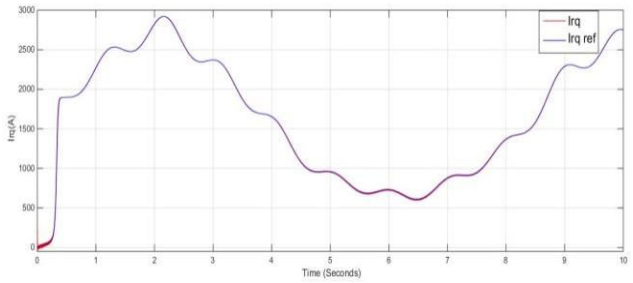

Figure-12. The direct rotor currents.

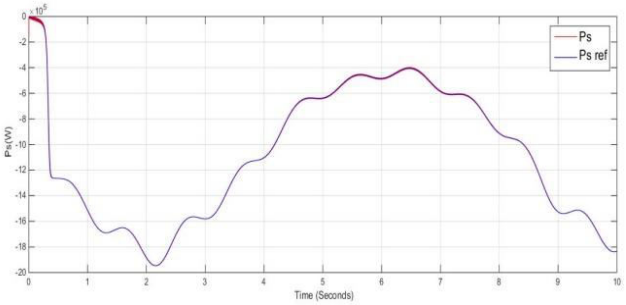

Figure-13. The active power of RSC.

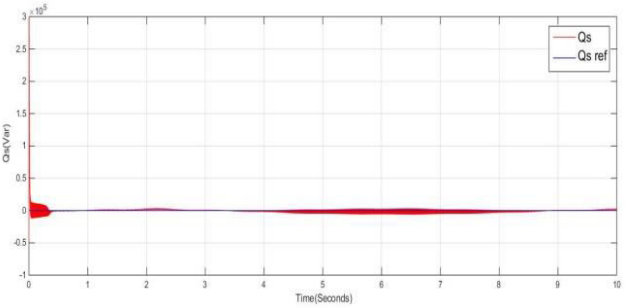

Figure-14. The reactive power of RSC.

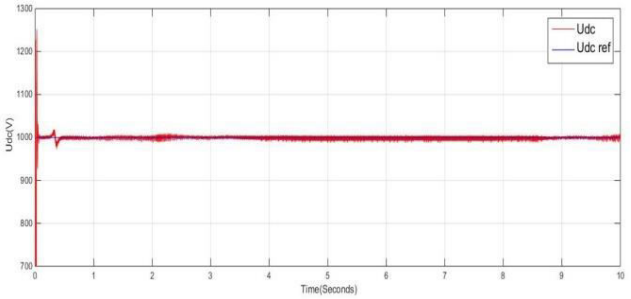

Figure-15. The U_{dc}voltage of the DC bus.

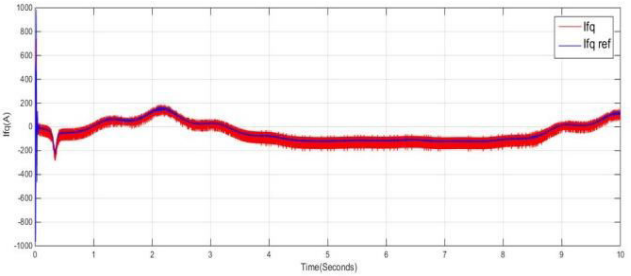

Figure-16. The quadrature currents of the filter.

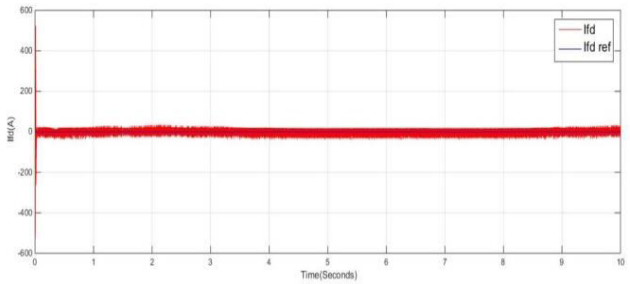

Figure-17. The direct currents of the filter.

5.2 Robustness test of the ADRC

In order to present the robustness of the ADRC control, it is necessary to vary the parameters of the model of DFIG and grid filter. In fact, the calculations of some regulators are based on functions whose parameters are assumed to be fixed. However, in a real system, these parameters are subject to variations caused by different physical phenomena.

To evaluate the performance of the ADRC controller, the value of the normal impedance of the filter and the rotor, as well as for the capacity of the DC bus, will be varied until to 150% of their values.

In this simulation, two impedance values of the gate filter (R*f*, L*f*) and the rotor (R*r*, L*r*) will be predefined; same thing for the DC bus capacity. The first $Z_{r,f,C}$ is the normal impedance; the second will be changed with 150%.

According to the results obtained in "Figures 18, 19, 20 and 21", which present the result of the rotor side control and the "Figures 22, 23, 24, 25 and 26" that presents the result of the grid side control, we notice that the variations of the internal parameters have almost no influence because of the regulators ADRC which makes it possible to compensate automatically the disturbances due to these variations. So the set point following is always guaranteed and stability of system is not affected.

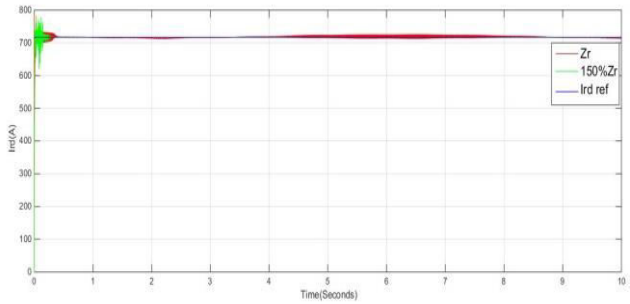

Figure-18. The direct rotor currents with variations parameters.

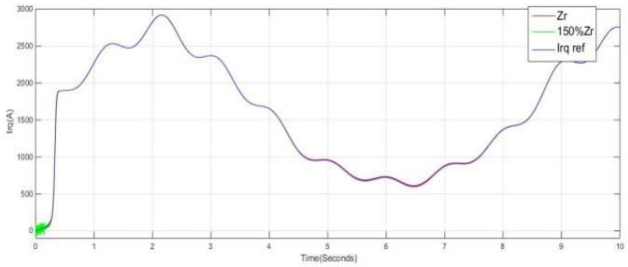

Figure-19. The quadrature rotor currents with variations parameters.

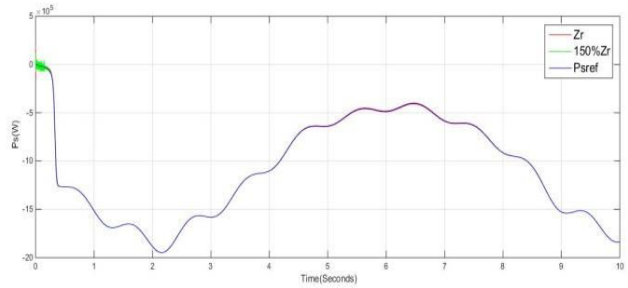

Figure-20. The Active power with variations parameters.

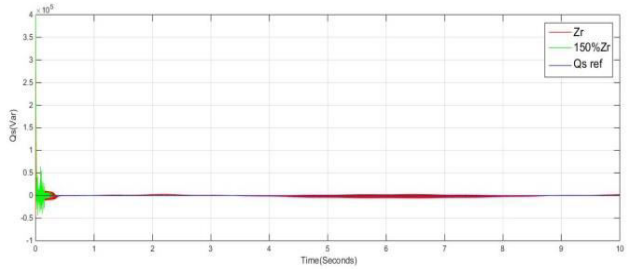

Figure-21. The Active power with variations parameters.

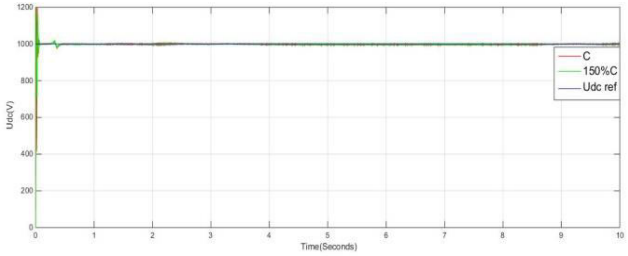

Figure-22. The U_{dc} Voltage with capacity variations.

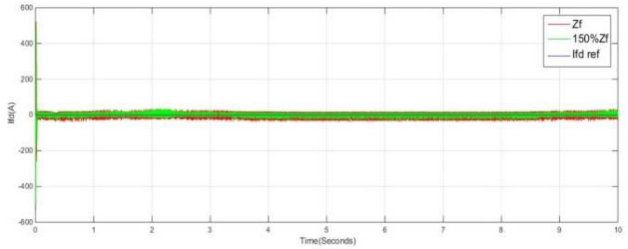

Figure-23. The direct filter currents with variations parameters.

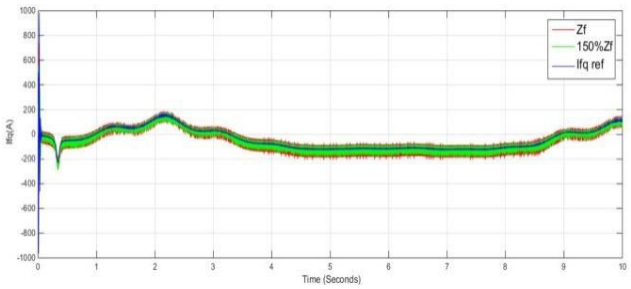

Figure-24. The quadrature filter currents with variations parameters.

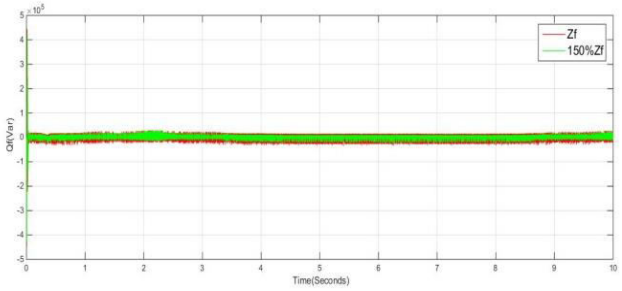

Figure-25. The filter reactive power with variations parameters.

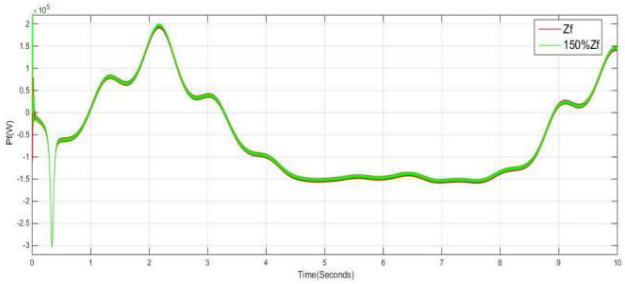

Figure-26. The filter active power with variations parameters.

6. CONCLUSIONS

In this article, we presented a method of the power control of the wind energy conversion system based on the DFIG. This control called ADRC makes it possible to extract a maximum power, to prohibit the exchange of reactive power with grid, and it is robust against the variations of the parameters. For that we did a simulation to test these performances.

This control is applied to the rotor and grid side power converter (RSC, GSC) through the rotor and filter currents.

The gains of the extended state observer (ESO) used in the ADRC control loop are chosen judiciously, and from the simulation results, which shows that the modeling errors are compensated and the signals of the physical quantities of the system follow their references, so the system is stable in spite of the changes of the parameters, this makes it possible to improve the efficiency of the wind turbine production.

Table-1. Parameters of DFIG.

Parameters	Value
Rated power Ps	2 Mw
Pole pairs p	2
Rotor resistance Rr	2.9 $10^{-3}\Omega$
Stator resistance Rs	2.6 $10^{-3}\Omega$
Mutual inductance M	2.5 10^{-3}H
Rotor inductance Lr	2.587 10^{-3}H
Stator inductance Ls	2.587 10^{-3}H

Table-2. Parameters of turbine.

Gearbox coefficient G	**92.6**
Moment of inertia **J**	1000 Kg/m^2
Viscous friction **f**	0.0024
Length of one blades **R**	40 m
Air density **ρ**	1.225 Kg/m^2

Table-3. The ADRC parameters.

K_p	200	K_{pc}	100	K_{pf}	250
β_1	3600	β_{1C}	1200	β_{1f}	2000
β_2	3240000	β_{2C}	360000	β_{2f}	1000000
b_0	$5.8454*10^3$	b_{C0}	$4.14*10^5$	b_{f0}	-400

REFERENCES

[1] R. Pena, J. Clare and G. Asher. 1996. A doubly fed induction generator using back-to-back PWM converters supplying an isolated load from a variable speed wind turbine. Electric Power Applications, IEE Proceedings. 143: 380-387.

[2] A. Boukhriss, A. Essadki and T. Nacer. 2012. Power control for a doubly fed induction generator. International Conference Complex Systems (ICCS).

[3] B. Betran, T. Ahmed-ali and M.E.H. Benbouzid. 2008.Sliding Mode PowerControl of Variable Speed Wind Energy Conversion systems. IEEE Transaction on energy conversion. 23(2).

[4] L. Pablo and U. Julio. 2005. Doubly Fed Induction Generator Model for transient Stability Analysis. IEEE Transaction on energy conversion. 20(2).

[5] B. Fredo, L. Marco and M. Ke. 2012.Power Electronics Converters for Wind turbine Systems. IEEE Transaction on industry applications. 48(2).

[6] A. Boukhriss, T. Nacer and A. Essadki.2013. A Linear Active Disturbance Rejection Control applied for DFIG based Wind Energy Conversion System. International Journal of Computer Science Issues (IJCSI).10(2):391-399.

[7] Z.Gao. 2003. Scaling and Bandwidth Parameterization Based Controller. Proceedings of the American Control Conference. 6: 4989-4996.

[8] H. Jingqing. 1998. Auto-Disturbance Rejection Control and its Applications. Control decision. 13(1):19-23.

[9] F. Poitiers, T. Bouaouiche, M. Machmoum. 2009. Advanced control of a doubly-fed induction generator for wind energy conversion. Electric Power Systems Research.79: 1085-1096.

[10] K. Eftichios and K. Kostas. 2006. Design of a maximum power tracking system for wind-energy-conversion applications. IEEE Transaction on industrial electronics. 53(2): 486-494.

[11] H. Gernot. 2013. A Simulative Study on Active Disturbance Rejection Control (ADRC) as a Control Tool for Practioners. Electronics. 2,246 279, doi:10.3390/electronics2030246.

[12] Q. Zheng, Z. Chen and Z. Gao. 2009. A practical approach to disturbance decoupling control. Control Engineering Practice. 17(9):1016-1025.

[13] R. Chakib, A. Essadki and M. Cherkaoui. 2014. Active Disturbance Rejection Control for Wind System Based On a DFIG. World Academy of Science, Engineering and Technology International Journal of Electrical, Computer, Energetic, Electronic and Communication Engineering. 8(8).